The Role of Solvent Structure in the Absorption Spectrum of Solvated Electrons: Mixed Quantum/Classical Simulations in Tetrahydrofuran (THF)

Michael J. Bedard-Hearn, Ross E. Larsen, and Benjamin J. Schwartz*

Department of Chemistry and Biochemistry
University of California, Los Angeles
Los Angeles, CA 90095-1569

Abstract: In polar fluids such as water and methanol, the peak of the solvated electron's absorption spectrum in the red has been assigned as a sum of transitions between an *s*-like ground state and three nearly degenerate *p*-like excited states bound in a quasi-spherical cavity. In contrast, in weakly polar solvents such as tetrahydrofuran (THF), the solvated electron has an absorption spectrum that peaks in the mid-infrared, but no definitive assignment has been offered about the origins of the spectrum or the underlying structure. In this paper, we present the results of adiabatic mixed quantum/classical molecular dynamics simulations of the solvated electron in THF, and proved a detailed explanation of the THF-solvated electron's absorption spectrum and electronic structure. Using a classical solvent model and a fully quantum mechanical excess electron, our simulations show that although the ground and first excited states are bound in a quasi-spherical cavity, a multitude of other, nearby solvent cavities support numerous, nearly degenerate, bound excited states that have little Franck-Condon overlap with the ground state. We show that these solvent cavities, which are partially polarized so that they act as electron trapping sites, are an inherent property of the way THF molecules pack in the liquid. The absorption spectrum is thus assigned to a sum of bound-to-bound transitions between a localized ground state and multiple disjoint excited states scattered throughout the fluid. Furthermore, we find that the usual spherical harmonic labels (e.g., *s*-like, *p*-like) are not good descriptors of the

* Corresponding author: schwartz@chem.ucla.edu

excited-state wave functions of the solvated electron in THF. Our observation of multiple disjoint excited states is consistent with femtosecond pump-probe experiments in the literature that suggest that photoexcitation of solvated electrons in THF causes them to relocalize into solvent cavities far from where they originated.

I. Introduction

Since their discovery over 40 years ago,[1] solvated electrons have been the subject of great interest: their large absorption cross-sections make them amenable to study by ultrafast spectroscopy,[2-5] and their simple electronic structure allows for detailed theoretical analysis via quantum simulation.[6-11] Figure 1 shows the optical absorption spectra of solvated electrons in several different solvents, reproduced from the Gaussian-Lorentzian fitting parameters given in Reference 12. For polar fluids such as water[7–9,13-15] and methanol,[16-18] the most widely accepted picture is that solvated electrons exist in a single quasi-spherical cavity that supports four bound eigenstates,[19] which resemble those of a particle in a spherical box. Many mixed quantum/classical simulations have supported to this idea, and the peak in the absorption spectrum has been assigned to transitions between an *s*-like ground state and three near-degenerate *p*-like excited states (although the extent to which this portion of the spectrum is inhomogeneously broadened remains an open question[20]). The blue tail of the absorption spectrum has been assigned to transitions between the ground state and a continuum of excited states that are delocalized throughout the fluid.[13,15,21,22]

However, a cavity picture is not necessarily expected to describe the behavior of solvated electrons in every solvent environment. In acetonitrile, for example, several groups have found evidence for two different types of solvated electrons with distinct absorption spectra: a cavity-

bound species that absorbs in the near IR, and a solvated molecular anion species that absorbs in the blue.[23-25] Moreover, in non-polar solvents such as liquid Xe,[26] liquid methane, and low density liquid ethane,[27] computer simulations have shown that the wave function of the solvated electron does not reside in a single cavity, but instead encompasses channels that run throughout the solvent. Excess electrons in these non-polar solvents do not absorb in the visible or near IR, which is consistent with the simulation picture of a highly delocalized ground state wave function and no bound electronic excited states. In the intermediate regime of weakly polar fluids such as tetrahydrofuran (THF) and other ethers, however, the solvated electron has an absorption spectrum, but it is quite different from that in polar fluids. Figure 1 and Reference 12 show that the peak of the solvated electron's spectrum in THF and other weakly polar fluids occurs at much lower energies and is substantially broader than the solvated electron's spectrum in water or methanol. The photochemistry of solvated electrons is also quite different in polar and weakly polar fluids. For example, Barbara and co-workers found that photoexciting hydrated electrons (created via multiphoton ionization of the solvent) near their absorption maximum led to little change in geminate recombination dynamics, implying that the excited states of the hydrated electron reside in the same, strongly polarized, solvent cavity as the ground state.[28] In contrast, Martini *et al*. found that photoexciting THF-solvated electrons (created via a charge-transfer-to-solvent excitation of Na) near their absorption maximum resulted in large differences in recombination dynamics, suggesting that photoexcited THF-solvated electrons *relocalize* into different solvent cavities.[29,30] Given these differences in spectroscopy and photochemical behavior, it is not clear whether or not the simple particle-in-a-spherical-cavity picture that applies in highly polar solvents is applicable to solvated electrons in either non-polar or weakly polar solvents.

All of this leads to the question of exactly how to think about solvated electrons in the intermediate regime of weakly polar fluids. Do the ground-to-excited-state transitions occur from a cavity-localized state or a delocalized state? Can the spectrum be assigned to a sum of bound-to-bound transitions or bound-to-continuum transitions? Do the wave functions of solvated electrons in weakly polar fluids encompass multiple solvent molecules or perhaps multiple solvent cavities and channels? Moreover, why is the spectrum of the solvated electron in hexamethylphosphoramide (HMPA), a polar fluid with a dielectric constant of ~30, so similar to that of the solvated electron in THF, which has a dielectric constant of only ~7.5 (*cf*. Figure 1)?[31] As we are aware of no previous simulations studying the properties of solvated electrons in weakly polar fluids, the purpose of this paper is to address the nature of solvated electrons in such liquids using mixed quantum/classical computer simulation.

In this paper, we present the results of mixed quantum/classical molecular dynamics simulations of the solvated electron in THF and offer a detailed assignment of the THF-solvated electron's absorption spectrum. We show how the solvent structure, particularly THF's ability to form transient cavities, determines how electrons behave in THF. We find that the reason the solvated electron's absorption spectrum in THF differs from that in water is because the THF solvent structure is naturally characterized by large spatial voids and deep potential energy traps, which do not exist in water. Our simulations show that the ground-state solvated electron in THF is indeed cavity bound, but that several of the excited states, although localized, have most or all of their charge densities in different cavities than the ground state. We will refer to the cavity that holds the ground state electron the *primary* cavity to distinguish it from the other, *disjoint* or *secondary* cavities that are occupied by the excited states. We will argue that the absorption spectrum of the THF-solvated electron thus consists of a superposition of strong

transitions from the ground state to excited states that occur the primary cavity, and weak transitions (due to poor spatial overlap) from the ground state to the many bound excited states that occupy the disjoint cavities. We also will speculate that the similarity of the spectra of solvated electrons in THF and HMPA results from the solvent packing in HMPA, which also has been characterized as having spatial voids.[32] Finally, we note that the presence of disjoint excited states also can explain why photoexcited electrons in THF undergo significant relocalization even though photoexcited electrons in water do not. Overall, the simulation results suggest that in weakly polar liquids, solvent structure and packing properties have a greater influence on the behavior of solvated electrons than any other single parameter, such as solvent polarity.

II. Computational Methods

All of the mixed-quantum/classical molecular dynamics (MD) simulations discussed here are equilibrium, adiabatic simulations of a single quantum particle (the excess electron) and 255 classical THF solvent molecules in a cubic box of side 32.5 Å, corresponding to the room temperature experimental solvent density of 0.89 g/cc. The classical solvent molecules are described by a 5-site, rigid and planar model for THF developed by Chandrasekhar and Jorgensen whose potential includes pair-wise additive Coulomb and Lennard-Jones (L-J) terms (see Table I);[33] we have explored the behavior of this classical model of THF in detail in a previous publication.[34] Our simulations employed the minimum image convention, and we used the position Verlet algorithm[35] with a 4-fs time step to integrate the classical equations of motion (including the Hellman-Feynman force from the electron, see Eq. 2, below). We used a modified SHAKE algorithm[36] to keep the THF molecules rigid and planar. The simulations were

performed in the microcanonical ensemble with the total energy conserved at all times to better than 0.005%. The average temperature of the system was 309 ± 7 K. The starting configuration was taken from an equilibrated all-classical simulation with a single negatively charged Lennard-Jones atom (σ = 5 Å, ε= $\varepsilon_{\text{oxygen}}$, see Table I). Once the L–J atom was removed, the system was equilibrated with the excess electron for an additional ~10 ps, and statistics were collected for another 32.5 ps.

The interaction between each classical THF molecule and the quantum mechanical electron was described with a pseudopotential, $V(\{\mathbf{r}\})$, whose form is an extension of that used in Liu and Berne's simulations of the solvated electron in ethane:[27]

$$\frac{V(\{\mathbf{r}\},\mathbf{r}_e)}{S(\{\mathbf{r}\},\mathbf{r}_e)} = \sum_{i=1}^{5} A_i^{(1)} e^{-B_i^{(1)}|\mathbf{r}_i-\mathbf{r}_e|} + A_i^{(2)} e^{-B_i^{(2)}|\mathbf{r}_i-\mathbf{r}_e|} + \frac{\alpha_i}{2|\mathbf{r}_i-\mathbf{r}_e|^4}\left(1-e^{(|\mathbf{r}_i-\mathbf{r}_e|/r_0)}\right)^6 - \frac{q_i}{|\mathbf{r}_i-\mathbf{r}_e|}T_i\left(|\mathbf{r}_i-\mathbf{r}_e|\right) + \sum_{j=1}^{5}\left[A_j^{(1)} e^{-B_j^{(1)}|\mathbf{r}_j-\mathbf{r}_e|}\right] \quad , \quad (1)$$

$$\frac{T_i(r)}{r} = \begin{cases} \dfrac{1}{r} & \text{if} \quad \dfrac{\alpha_i}{2} + 0.1\text{ Å} < r \\ ar^3 + br^2 + cr + d & \text{if} \quad \dfrac{\alpha_i}{2} < r < \dfrac{\alpha_i}{2} + 0.1\text{ Å} \\ mr & \text{if} \quad \dfrac{\alpha_i}{2} > r \end{cases}$$

where the sum on i runs over the 5 solvent sites and the sum on j runs over the mass-weighted centers of the 5 intramolecular bonds. The coefficients A_i represent the strength of the interaction of each THF site with the electron; the coefficients B_i provide an effective size for how each solvent site interacts with the electron. The set $\{\mathbf{r}\}$ refers to the site positions of a specific THF molecule, and $\mathbf{r}_i$, $\mathbf{r}_j$ and $\mathbf{r}_e$ are the positions of the classical solvent sites, the mass-weighted bond mid-points, and the electron, respectively. The function $S(\{\mathbf{r}\})$ is a function developed by Steinhauser,[37] which tapers the total pseudopotential smoothly to zero for electron-

solvent center-of-mass distances between 15.75 Å and 16.25 Å (half the box length). The A_i coefficients for each solvent site, i, are chosen so that the first term in Eq. 1 is attractive and the second term is repulsive; α in the third term represents the site polarizibility. The fourth term in Eq. 1 is the Coulomb interaction between the excess electron and the classical partial charges on the oxygen and α-methylene sites of the THF molecules, and $T_i(r)$ cubically tapers this interaction smoothly to zero, in accord with Gauss' Law. The final term in Eq. 1, which is summed over the bond centers rather than the solvent sites, is purely repulsive, representing Coulomb and exchange repulsion between the excess electron and the solvent molecule's bonding electrons. The parameters for $T_i(r)$ are site-specific and depend on the Lennard-Jones diameter (σ) of each solvent site; we used a simple matrix inversion to solve for the coefficients a, b, c, and d to ensure that both $V(r)$ and its first derivative were continuous. All of the parameters used in our electron-THF pseudopotential are summarized in Table I.

In addition to using five solvent sites and five bonds and adding the Coulomb term, we made the following changes to the electron-ethane pseudopotential of Liu and Berne[27] to better represent the interaction of the solvated electron with THF:

(a) We scaled the parameters $B_j^{(i)}$ from Liu and Berne's model for CH_3 sites to better represent the sizes of oxygen and CH_2. The scaling factor we chose was the ratio of the L–J diameter (σ) for CH_3[38] with the L–J diameter for each oxygen and CH_2 site in our classical THF model.[33]

(b) We changed the polarizability, α, of the oxygen site to better represent the electron's interaction with the solvent oxygen so that it was roughly half way between the polarizability of oxygen in a water molecule[39] and atomic oxygen.[31]

(c) For the Oxygen-β-methylene bond midpoints, we chose the mass-weighted midpoints instead of the geometric midpoints.

For each solvent configuration, the pseudopotential from all 255 classical solvent molecules was evaluated on a uniformly-spaced $24 \times 24 \times 24$ grid spanning the entire simulation cell. The time-independent Schrödinger equation for the quantum electron was then solved on this grid using an iterative and block Lanczos routine.[40] We evaluated the kinetic energy operator in Fourier space, using the MFFT package to perform the forward and reverse transforms.[41] To better isolate the bound eigenstates in the Lanczos routine, we employed an exponential spectral filter using a split operator.[40] At each time step, we calculated the lowest seven eigenvalues and eigenvectors. Finally, the force that the quantum electron exerts on the classical particles was calculated using the Hellman-Feynman theorem:[42]

$$\mathbf{F}_r = -\langle \psi | \vec{\nabla}_r \hat{H} | \psi \rangle, \tag{2}$$

where $|\psi\rangle$ is the wave function of the electronic ground state and $\vec{\nabla}_r$ is the gradient with respect to the solvent positions, r. Further details of the way our group performs mixed-quantum/classical simulations can be found in References 43 and 44, and more complete details of these particular simulations, as well as a comparison of this modified pseudopotential with a rigorous THF pseudopotential, will be provided in a future publication.[45]

III. Results

Figure 2a shows the dynamical history of the adiabatic eigenenergies of the solvated electron in THF over a short portion of the 32.5-ps equilibrium trajectory; the eigenenergies fluctuate due to motions of the surrounding solvent molecules. Despite the fact that the ground state energy of the solvated electron in THF (–2.1 eV) lies slightly higher than that of the

solvated electron in methanol (–2.2 eV),[17,46] and significantly higher than in water (–3.1 eV)[47] the solvated electron in THF has seven or more clearly defined solvent-supported bound states, in marked contrast to only four distinct bound states observed in water and methanol.[19] Figures 3a and 3b show the calculated absorption spectrum (discussed below) and density of energy gaps averaged over the entire 32.5-ps trajectory. The density of energy gaps is calculated as a histogram of the instantaneous energy gaps from the ground state to each of the six excited states. Unlike what is observed for the hydrated electron, Fig. 3 shows that in THF, the absorption spectrum and density of energy gaps are remarkably different. In water, the transitions to the first three excited states have nearly identical oscillator strengths, so the density of gaps and the absorption spectrum are nearly identical for the bound-to-bound transitions.[21,22]

What causes the solvated electron to behave so differently in THF and in water? Figure 4 displays the charge densities (wire mesh plots) for the first seven eigenstates of the solvated electron in THF for thesingle selected solvent configuration that is denoted by the arrows in Figs. 2. Panel (a) of Figure 4 shows that like the hydrated electron, the ground state of the THF-solvated electron occupies a large, quasi-spherical cavity, but we find that it is slightly larger and more aspherical than that in water. In THF, the average radius of gyration of the ground state of the solvated electron is 2.85 Å, whereas simulations of the hydrated electron yield a radius of gyration of 2.42 Å,[47] similar to the radius of 2.5 Å determined from moment analysis of the experimental absorption spectrum.[48] Moreover, the average ratio of the maximum to the minimum principle moments of inertia (I_{max}/I_{min}) of the THF-solvated electron is 1.4, compared to only 1.2 for the hydrated electron.[44]

Although the ground state of the THF-solvated electron is larger and somewhat less spherical than that of the hydrated electron, the most dramatic differences between the two types

of solvated electron are found in the nature of the electronic excited states. The colored wire meshes in Figure 4 show contours at 10% of the maximum charge density for each of the eigenstates. To aid in the 3-D perspective, we have placed uniformly–sized drop shadows under the center of mass of each state. Panels (b), (c), and (d) of Figure 4 show that the first three excited states (panel (d) also shows the fifth excited state in blue) of the THF-solvated electron are not all *p*-like states occupying the primary cavity, as is the case for solvated electrons in water and methanol. It is worth noting that the first and second excited states (panels (b) and (c)) have nodes that are not visible near the center of the primary cavity and that the lobes of the first excited state (panel (b)) are oriented along the long axis (into the page) of the aspherical primary cavity, as expected for a particle in an aspherical box. The rest of the excited states are either localized in other cavities (some as far away as 11 Å from the ground state[49]) or occupy multiple cavities, sometimes including the primary cavity. Panels (e) and (f) show two states (the fourth and sixth excited states) that fit the latter description: each of these states has charge density in two disjoint cavities as well as some in the primary cavity. The disjoint character of the solvated electron's excited states seen in this configuration is typical, as we have verified by examining dozens of uncorrelated configurations. We have further verified this behavior by investigating the transition dipole moments between the ground and excited states (Fig. 2b) and the degree of spherical symmetry (Fig. 2c), both of which we will discuss further below. Finally, of the higher-lying excited states above the first and second excited states, we find that most of the time, at least one of them (usually the third or fourth state) has some of its charge density in the primary cavity.

Why do the excited states of the solvated electron in THF have such an unusual disjoint structure? The answer lies in the fact that the disk-like solvent molecules pack in such a way as

to create a cavity-filled liquid that provides multiple traps in which to localize an excited solvated electron. Chandrasekhar and Jorgensen performed classical Monte Carlo simulations using this model of THF and suggested that the molecules tend to pack in chain-like structures.[33] These authors also examined a similar THF model that allowed for ring puckering, but found that the small distortions from planarity made no difference in the overall solvent packing.[33] Figure 4 shows the relationship between cavity trapping sites in the liquid and the electronic charge densities of the various THF-solvated electron eigenstates. To determine the location of the cavity traps in the solvent, we calculated the distance between each of the grid points (on which the Schrödinger equation was solved) and the nearest solvent site in any direction. We then defined a point as lying within a void if the distance to the nearest solvent site was ≥ 2.5 Å. To ensure that the solvent voids we examined were also potential energy traps for the electron, we required that the total value of the pseudopotential at each cavity-trapping site had to be less than –0.11 Hartree. In Figure 4, these cavity traps are shown as the orange surfaces. Figure 4 makes it clear that although the first two excited states are bound in the primary cavity containing the ground–state electron near the center of the simulation box, the other excited state wave functions have amplitude in one or more disjoint cavities. In fact, we have found that some of the disjoint secondary potential energy traps are deep enough to support more than one bound state.

To determine whether the existence of these secondary potential energy traps is induced by the presence of the electron in the primary cavity or is an inherent property of the liquid itself, we examined the trap structure of neat THF.[50] We find that there is always at least one trap somewhere in the neat THF simulation box that is large enough and deep enough to localize an electron. Furthermore, as we saw in the secondary cavities around THF-solvated electron, some

of the traps in the neat liquid are able to support two bound states, although most are not. But perhaps most importantly, we found that the distribution of traps seen in the neat liquid is essentially the same as that around the solvated electron, excluding the primary cavity. Figure 5 shows the distribution of energies for the three lowest eigenstates in the neat liquid (i.e. with no solvated electron present; red dashed curves) along with the distributions for the fourth, fifth, and sixth excited states of the THF-solvated electron system (solid black curves). Clearly, the distributions of energy for the three lowest states of an injected electron are identical to the energy distributions of the excited states of the equilibrated THF-electron system. This demonstrates that the disjoint nature of the THF-solvated electron excited states is indeed a natural property of the THF liquid structure. Thus, aside from the primary cavity, the THF-solvated electron seems to have little influence on the rest of the liquid structure: the nascent cavities in neat THF are the same as those in the THF-electron system, and it is these cavities that give rise to the disjoint excited states that in turn are responsible for the absorption spectrum, as we discuss below. This is why we say that the solvent structure controls the electronic structure of the solvated electron in weakly polar liquids. We note that investigations of pre-existing solvent traps have been performed for both neat water[51,52] and methanol,[53] although the number, depth, and size of the traps appear to be fewer and smaller than those in liquid THF. For example, an electron injected into neat water initially has no bound states,[54] whereas in neat THF, the six lowest states have eigenvalues below the vacuum level at least some of the time.

The disjoint nature of the THF-solvated electron's excited states shown in Fig. 4 allows us to assign the calculated absorption spectrum, $A(\omega)$, shown in Fig. 3a, which was calculated in the inhomogeneous limit by binning the transition dipole matrix elements between the ground and each of the first six excited states:[55]

$$A(\omega) = 4\pi^2\alpha\omega\sum_i \omega_{0i}\left|\langle 0|\mathbf{r}|i\rangle\right|^2 g(\omega-\omega_{0i}), \quad (3)$$

where α is the fine structure constant, 0 is the ground state and i is the final state, ω is the eigenvalue, $\omega_{0i} = \omega_i - \omega_0$, and the bin size was 0.075 eV. The individual transitions between the ground state and each of the six excited states underlying the total absorption spectrum are shown as the thin grey and black curves. The width of the calculated absorption spectrum of the THF-solvated electron agrees well with the experimental spectrum shown in Fig. 1. The calculated absorption maximum, however, is blue-shifted a few tenths of an eV from experiment, which is perhaps not surprising given the relative simplicity of our pseudopotential and the lack of solvent polarizability in our model of THF.[56]

We assign the absorption spectrum of the THF-solvated electron to a sum of strong transitions from the ground to the first and second excited states, plus a multitude of weak transitions from the ground state to the higher excited states. Figure 3a shows that the transitions from the ground state to the first three states have comparable (but unequal) oscillator strengths and make up the bulk of the spectrum near the absorption maximum. Figure 2b shows that absorption to the second excited state (solid black curve) occasionally has a very low transition dipole moment. We find that these instances of a low transition dipole moment from the ground to second excited state correlate with configurations where the majority of the second excited state's charge density is outside of the primary cavity. Furthermore, Figures 2b and 3a show that the oscillator strengths of the transitions to the third and higher states decrease with increasing energy because only part (or in some cases, none) of the relevant excited-state wave functions reside in the primary cavity. This lack of Franck-Condon overlap between the ground and excited states explains why the absorption spectrum (Fig. 3a) does not resemble the density of

energy gaps for the bound states (Fig. 3b),[57] and provides an assignment for the relatively weak absorption in the blue tail of the THF-solvated electron's spectrum. By studying the behavior of the transition dipole moments over the entire 32.5-ps trajectory, we find that most of the time, only the first and second excited states lie entirely within the primary cavity. All of the other transitions that compose the absorption spectrum occur to states occupying disjoint or multiple cavities.

Figure 2 also makes it clear that solvent motions cause all of the excited states, not just the high-lying states, to undergo many avoided crossings. This can be seen by noting that the near-degeneracies in the adiabatic energy levels (Fig. 2a) occur at precisely the same times as the step-function changes in the transition dipole moments (Fig. 2b). The ground state of the THF-solvated electron lies in its primary cavity, which often contains two (and occasionally three) bound excited states. Higher-lying excited states largely occupy other cavities that would be present whether or not there was a solvated electron nearby. The energies of these excited states depend on the relative depth of the traps in each of the secondary cavities, and as solvent fluctuations change the relative sizes and depths of secondary cavities, the energy ordering of the states that occupy these cavities can change, even though the extent of the overlap these states have with the ground state may not.

The next question we address is how well the language of spherical harmonics, borrowed from the description of solvated electrons in water[22] and methanol,[15] works for understanding the nature of the electronic states of the solvated electron in THF. We have investigated the spherical symmetry of the THF-solvated electron eigenstates using a method developed by Sheu and Rossky[58] to calculate the projection of each state onto the spherical harmonics, choosing the origin at the ground-state center of mass (see Appendix). Figure 2c shows the spherical

harmonic projections as a function of time, and Table II summarizes the projection results for solvated electrons in both THF and water.[59] We find that on average, the THF-solvated electron's ground state has 81% *s*-like character, comparable to the 82% *s*-like character of the ground-state hydrated electron. However, the first three excited states of the THF-solvated electron are only 67%, 53% and 31% *p*-like, respectively, much smaller than the first three excited states in water, which are all more than 70% *p*-like. The third excited state in THF also exhibits 17% *d*-like character, and we attribute this nearly complete lack of spherical symmetry to the fact that the third excited state of the THF-solvated electron tends to be the lowest state that regularly occupies a disjoint cavity. Furthermore, given that it almost always resides in the primary cavity, the second excited state of the THF-solvated electron has surprisingly little *p*-like character compared to any of the bound excited states in water or even to the THF-solvated electron's own first excited state.

To better understand the lack of *p*-like symmetry in the second excited state, we define that a state is of a particular symmetry when its projection onto the relevant set of spherical harmonics is greater than 67%. By doing this, we can calculate the amount of time that each state is *s*-like, *p*-like, or *d*-like, and this information is summarized in Table II as the "time average." Table II and Figure 2c make it clear that the reason the second excited state has so little *p*-like character is due both to the asphericity of the primary cavity and to avoided crossing events with the third excited state. One need only look at the crossings between 1.25 and 1.5 ps in Fig. 2, for example, where the second excited state (solid black curve) at 1.30 ps is mostly *p*-like in character, but crosses with the third excited state (solid grey curve) at 1.34 ps. The result of this curve crossing is that the second excited state no longer occupies the primary cavity, thus removing any Franck-Condon overlap with the ground state (Fig. 2b) and any hope of being

spherically symmetric around the center of mass of the ground state (Fig. 2c). After a few time steps (at 1.45 ps), the primary cavity changes shape again (or perhaps the disjoint cavity closes up), causing the second state to reside back in the primary cavity with mostly *p*-like symmetry, while the third state returns to its disjoint cavity. The slight difference between the low-energy edge of the distribution of energy gaps of the neat THF ground state and the fourth THF-solvated electron excited state in Figure 5 also can be explained by curve-crossings. The numerous crossings of the third and fourth excited states cause the fourth excited state of THF-solvated electron to sometimes occupy the primary cavity rather than the lowest-energy secondary cavity.

Finally, although the nature of the disjoint excited states depends primarily on solvent packing, we note that solvent structure alone cannot account for all of the electronic properties in this system. To find out exactly how much stabilization is provided by THF's weak dipole, we took several hundred configurations from the 32.5-ps equilibrium solvated electron trajectory and solved the Schrodinger equation using the pseudopotential in (Eq. 1) without the Coulomb terms. With all other things being equal (including the presence of the large primary cavity), this test shows how well the void structure of THF could solvate an excess electron without the addition of Coulomb stabilization. The difference between the average energy of the ground state in these calculations and the average energy of the ground state using the full pseudopotential was approximately +2 eV. The secondary cavities were typically unable to bind the excited states without the Coulomb interaction, but in a few cases where the first two states had eigenvalues below the vacuum level, we did see cavity-bound eigenstates in the secondary cavities.

Overall, even though THF is not as polar as water or methanol, the dipolar interactions do provide a significant amount of stability to the solvated electron. However, these energetic

considerations must be understood in context with the solvent structure to fully explain the nature of the solvated electron. The THF-solvated electron strongly influences the local polarization of the primary cavity, yet secondary cavities, which do not contain any ground-state charge density, are also attractive. This means that the nascent cavities in neat THF (and therefore the secondary cavities in the THF-electron system) must be at least partially polarized, since they can support one or more bound states (*cf.* Fig. 5). The difference between the two types of cavities is that the ground-state THF-solvated electron exists in a permanent and strongly polarized cavity, while the secondary cavities are transient and less attractive. This idea that the secondary cavities are partially polarized is further supported by the fact that when we turn off the Coulomb parts of the pseudopotential, only the ground state (which still usually resides in the primary cavity) and occasionally the first excited state (usually in a secondary cavity) remain bound.

IV. Discussion

In summary, we have used mixed-quantum/classical MD simulations to calculate the properties of solvated electrons in the weakly polar fluid THF. By examining the transition dipole moments and visualizing the solvent cavities and potential energy traps, we have shown that the absorption spectrum of solvated electrons in THF is composed of multiple low-energy bound-to-bound transitions. The excited states of the THF-solvated electron, however, lack the quasi-spherical symmetry seen in simulations of the hydrated electron. Thus, the important feature of these transitions is that although some of them occur to states within the same cavity, the majority of them do not. We have shown that solvent fluctuations continuously modify the size, shape, and attractiveness of the secondary cavities, which in turn modify the nature and

energies of the excited states. Our multiple cavity picture explains why solvated electrons in THF have such a broad, featureless absorption spectrum.

As we have argued throughout this paper, the THF-solvated electron's absorption spectrum results primarily from the presence of multiple potential energy traps, and is not a direct consequence of the weak polarity of the solvent. This suggests that a solvated electron in any fluid that has large cavities should have a similar absorption spectrum. Indeed, Figure 1 shows that the solvated electron in the polar solvent HMPA, which has nearly the same dielectric constant as methanol,[31] has a very similar absorption spectrum to that of the solvated electron in weakly polar THF. It is believed that the diffuse nature of the positive end of the HMPA dipole leads to poor packing of the HMPA molecules, so that the HMPA liquid structure also may be characterized by voids,[32] and this could explain the similarity of the spectra of the two different types of solvated electron.

We also have shown that in weakly polar liquids like THF, packing considerations can outweigh polarity in determining essential properties of solvated electrons. This picture is consistent with studies of the nature of solvated electrons in non-polar liquids such as He[26] and ethane.[27] He atoms pack efficiently in the liquid, so that even though He is a non-polar fluid, there are no nearby traps to support disjoint excited states. The ground state of the solvated electron in liquid He forms a cavity due to Pauli repulsion, and the lack of nuclear polarization makes the cavity deep enough to support only a single electronic ground state.[26] In liquid ethane, Liu and Berne used mixed quantum/classical simulations to explain the experimental density dependence of solvated electrons.[27] Although at low solvent densities the electron is delocalized, at high densities, these workers found that the electron was trapped in a single cavity. They explained this by noting that at high densities, there is a change in the solvent structure that

closes the channels available to the electron at low densities. Finally, we note that although traps and voids do exist in liquid water[52] and methanol,[51] the depth of such traps is so shallow relative to the depth of the highly-polarized primary cavity that any disjoint excited states play relatively little role in the spectroscopy of the solvated electron in these polar liquids.

The presence of the disjoint excited states observed in our simulations is supported by three-pulse femtosecond optical control experiments on solvated electrons in THF. Martini, Barthel and Schwartz showed that after creation of a THF-solvated electron via photodetachment using the charge-transfer-to-solvent transition of the sodium anion, re-excitation of the solvated electron could either enhance or suppress the rate of back electron transfer to the parent sodium atom, depending on the time at which the electron was re-excited.[29,30] These changes in recombination dynamics were explained by a model in which the re-excitation pulse delocalizes electrons throughout the solvent, so that when the electrons return to their electronic ground state, some of them do so in cavities far from where they had originated. Our simulations are consistent with this picture, as one can imagine that following excitation to one of the disjoint excited states, the non-adiabatic transition that returns the electron to its ground state could do so into any of the secondary cavities, effectively relocalizing the electron. Non-adiabatic simulations of this process that will directly test this postulate are presently underway in our group.[45] Similar experiments by Barbara and co-workers studying the recombination of electrons in water with their parent hydronium ions/hydroxyl radicals saw much less of an effect, consistent with the idea that the bound excited states of the hydrated electron are localized in the primary cavity and have little or no disjoint character.[60]

Overall, it is clear that the nature of solvated electrons is significantly different in THF than in polar fluids such as water or methanol. We attribute this difference to the many pre-

existing attractive solvent cavities that are inherent to the structure of liquid THF. Due to their disk-like nature, the THF solvent molecules are unable to pack efficiently, thus creating the spatial voids. Moreover, the voids in neat THF are not merely vacancies, but some are partially-polarized cavities that can act as electron trapping sites. These attractive voids account for the presence of bound excited states that are spatially separated from the ground state, which results in little transition dipole moment between them. Furthermore, since the secondary cavities are inherent to the solvent structure (*cf*. Fig. 5) and are close in energy to the ground state, the solvated electron's absorption spectrum in THF is red-shifted relative to the absorption spectrum in most strongly polar solvents. Of course the nature of the solvated electron in liquids can be traced back to a combination of electrostatic interactions and solvent structure, but we have shown that THF's inability to pack efficiently creates partially-polarized cavities, leading to a number of unusual solvated electron behaviors not seen previously in simulation.

Acknowledgments

This work was supported by a grant from the National Science Foundation (CHE-0240776). The authors would like to thank C. Jay Smallwood for helping to modify the electron-THF pseudopotential. The images in Figure 4 were created using the UCSF Chimera package from the Computer Graphics Laboratory, University of California, San Francisco (supported by NIH P41 RR-01081).[61]

Appendix

To calculate the projections of the solvated electron wave functions onto the spherical harmonics, we used the method outlined by Sheu and Rossky in Ref. 58. Briefly, the amount of

overlap of an eigenstate, ψ, with a particular spherical harmonic, Y_{lm}, with both represented on a finite and discrete grid is calculated as

$$P_{lm} = \frac{1}{\pi} \int_0^{\infty} dk \left[\left[\int d\tau Y_{lm}(r) \frac{\cos kr}{r} \right]^2 + \left[\int d\tau Y_{lm}(r) \frac{\sin kr}{r} \right]^2 \right], \qquad \text{(A1)}$$

where the integrals over τ are integrals over the volume of the simulation cell, and the limits on the integral over k need go only from the inverse of the longest wavelength sampled by the simulation cell (the distance along the diagonal of the simulation cell) to the inverse of shortest wavelength sampled by the grid (the shortest distance between any two co-linear grid points). In the work presented above, we used a Simpson' Rule integrator with wavevectors defined by the long diagonal of the simulation box: $\Delta k = k_{min} = \pi/(2L\sqrt{3})$, $k_{max} = N\pi/(2L\sqrt{3})$, where $N = 24$ is the number of grid points in one dimension and $L = 16.25$ Å (half of the length of one side of the simulation box). Each of the projections presented in Table II and Figure 2c was calculated as the sum over all m for $l = 0$, 1, or 2. Because the simulation cell for water was much smaller (~18.2 Å / side) than in THF (32.5 Å / side), we used a 16^3 grid instead of a 24^3 grid for the projections of the hydrated electron to yield comparable grid spacings (1.13 Å in water, 1.33 Å in THF).

Relative to the data presented in this paper, Sheu and Rossky performed their calculations on a very dense grid (32^3 grid points in a box of side 24.66 Å). Therefore, in order to test the accuracy of our projections, we performed test calculations by examining the projections of the first 16 spherical harmonics onto various functions, including Gaussians of different widths, and hydrogenic orbitals, all expressed on our 24^3 grid. We found that Gaussians and the hydrogenic 2*s*- and 2*p*-orbitals all had unambiguous projections of approximately 95% onto their respective spherical harmonics, and were orthogonal (overlap < 10^{-31} %) to the other spherical harmonics.

The only exception was the projection of the hyrdogenic 2*p*-orbitals onto the $l = 3$ (*f*-like) spherical harmonics, which was ~8%, but as expected, this projection decreased to 0.3% when we doubled the grid density. The $3d_{z2}$ hydrogenic orbital on the 24^3 grid had ~80% overlap with the $l = 2$ spherical harmonics, and a small projection (less than 8%) onto the $l = 3$ spherical harmonics.

Table I – Parameters for the classical THF solvent potential (Lennard-Jones plus Coulomb), taken from Ref. 33, and the quantum THF-electron pseudopotential (Eq. 1), which was modified from the hydrocarbon pseudopotential presented in Ref. 27.

				Quantum Pseudopotential				
Solvent Site	Classical Potential							
	σ / Å	**ε / J x 10-21**	**q / e**	**A1 / a.u.**	**A2 / a.u.**	**B1 / Å^{-1}**	**B2 / Å^{-1}**	**α / a.u.**
Oxygen	3.000	1.18	-0.5	300	-132	4.99	4.44	7.71
α-methyl	3.800	0.82	0.25	300	-132	3.95	3.52	17.5
β-methyl	3.905	0.82	--	300	-132	3.84	3.42	17.5
midpoint	--	--	--	165	--	3.78	--	--

Table II – Results for the projections of the wave functions of solvated electrons in THF and water onto the spherical harmonics (Eq. A1). The projections of the THF-solvated electron were calculated from configurations spanning 18.5 ps of the total equilibrium trajectory, and the projections for the hydrated electron were calculated from configurations spanning a 4.5-ps run.[59] In all cases except the "time average", the two standard deviation error bars are less than 1%. The "time average" is the fraction of time each state is projected more than $^2/_3$ onto its maximally projected spherical harmonic (the maximally projected spherical harmonics are shown in bold face). That is, the second excited state of the solvated electron in THF has a $^2/_3$ projection onto the $l = 1$ spherical harmonics only 17% of the time, meaning that it meets our criterion for being *p*-like only 17% of the time. The one-standard-deviation error bars for the time averages are given in parentheses.

THF state	s	p	d	Time average
0	**81**	4	3	100
1	2	**67**	8	59 (10)
2	2	**53**	15	17 (7)
3	5	**31**	17	3 (3)
4	5	**19**	17	2 (2)
5	5	**16**	15	1 (0.5)
6	4	11	**14**	0

Water state	s	p	d	Time average
0	**82**	5	1	100
1	3	**77**	7	93 (3)
2	2	**75**	8	89 (4)
3	2	**73**	9	84 (5)

Figure 1 – Gausssian-Lorentzian fits to the absorption spectra of the solvated electron in THF (solid curve), HMPA (dashed curve), water (dash-dot curve), and methanol (dotted curve). The fitting parameters were taken from Ref. 12.

Figure 2 – Time dependence of (a) the eigenvalues, (b) the transition dipole moments, and (c) the spherical harmonic projections of the lowest 6 eigenstates of the THF-solvated electron shown over a small window in the middle of our 32.5-ps equilibrium trajectory. The key for panel (b) should be read as the transition from the ground state (labeled as 0) to the i^{th} excited state; $\square_i$ is the energy of state i and $\square_0$ is the energy gap between the ground state and the i^{th} state. The projection (see the Appendix and Ref. 58) of each excited eigenfunction onto the $l = 1$ (p-like) spherical harmonic is shown, as is the projection of the ground state is onto the $l = 0$ (s-like) spherical harmonic. The spherical harmonic projection of the sixth excited state is not shown in panel (c) because this state has no significant spherical symmetry. The arrows indicate the specific configuration examined in Fig. 4.

Figure 3 – (a) Calculated absorption spectrum for an excess electron in THF using Eq. 3. Underlying the total spectrum (thick black curve) are the individual transitions from the ground to each of the excited states (thin grey curves). (b) The scaled density of energy gaps of the THF-solvated electron between the ground and each of the six lowest excited states, defined as the distribution of instantaneous energy gaps between the ground and each of the excited states.

Figure 4 – Attractive cavities (orange surfaces) and charge densities (wire meshes) for the solvated electron in THF, calculated as described in the text. The wire meshes shown are

contours drawn at 10% of the maximum charge density. Panel (a) shows the ground state, (b) the first excited state, (c) the second excited state (d) the third (red) and fifth (blue) exited states, (e) the fourth excited state, and (f) the sixth excited state. The drop shadows are placed under each state's center of mass are to aid in perspective and are not meant to convey size information.

Figure 5 – Comparison between the normalized distributions of energy for the equilibrated THF-solvated electron eigenstates (black solid curves) and for the eigenstates of an excess electron injected into neat THF (red dashed curves). The energy probability distributions in the neat liquid were calculated from an 8-ps trajectory, whereas the distributions for the solvated electron were calculated from the full 32.5-ps equilibrium trajectory.

References:

1 E. J. Hart, J. W. Boag, J. Am. Chem. Soc. **84**, 4090 (1962).

2 M. S. Pshenichnikov, A. Baltuska, D. A. Wiersma, Chem. Phys. Lett. **389**(1-3), 171 (2004).

3 C. Silva, P. K. Walhout, P. J. Reid, P. F. Barbara, J. Phys. Chem. A **102**(28), 5701 (1998).

4 X. L. Shi, F. H. Long, K. B. Eisenthal, J. Phys. Chem. **99**(18), 6917 (1995).

5 M. Assel , R. Laenen, A. Laubereau, J. Chem. Phys. **111**(15), 6869 (1999).

6 K. Leung, D. Chandler, Ann. Rev. Phys. Chem. **45**, 557 (1994).

7 K. F. Wong, P. J. Rossky, J. Chem. Phys. **116**(19), 8418 (2002).

8 P. J. Rossky, J. Schnitker, J. Phys. Chem. **92**(15), 4277 (1988).

9 E. Neria, A. Nitzan, R. N. Barnett, U. Landman, Phys. Rev. Lett. **67**(8), 1011 (1991).

10 D. F. Coker, B. J. Berne, D. J. Thirumalai, Chem. Phys. **86**(10), 5689 (1987).

11 K. F. Wong, P. J. Rossky, J. Phys. Chem. A **105**(12), 2546 (2001).

12 F.-Y. Jou, G. R. Freeman, J. Phys. Chem. **81**(9) 909 (1977).

13 B. J. Schwartz, P. J. Rossky J., Chem. Phys. **101**(8), 6902 (1994).

14 C. Nicolas, A. Boutin, B. Lévy, D. J. Borgis, Chem. Phys. **118**(21), 9689 (2003).

15 P. J. Rossky; J. Schnitker, J. Phys. Chem. **92**, 4277 (1988).

16 P. Minary, L. Turi, P. J. Rossky, J. Chem. Phys. **110**(22), 10953 (1999).

17 J. Zhu, R. I. Cukier, J. Chem. Phys. **98**(7), 5679 (1993).

18 L. Turi, A. Mosyak, P. J. Rossky, J. Chem. Phys. **107**(6), 1970 (1997).

19 In both water and methanol, these states are all localized in the same cavity, even though the energies of the higher-lying excited states sometimes fluctuate above the vacuum level; this is more pronounced for some methanol models, with the 3rd excited state never fluctuating below the vacuum level (Ref. 16). However, we refer to them as “bound” states since they are well confined to the same solvent cavity as the ground state and are not delocalized throughout the solvent.

20 M. C. Cavanagh, I. B. Martini, B. J. Schwartz, Chem. Phys. Lett. **396**(4-6), 359 (2004).

21 B. J. Schwartz and P. J. Rossky, J. Chem. Phys. **101**, 6917 (1994).

22 J. Schnikter, K. Motakabbir, P. J. Rossky; R. Friesner, Phys. Rev. Lett. **60**(5), 456 (1988).

23 M. Mitsui, N. Ando, S. Kokubo, A. Nakajima, K. Kaya, Phys. Rev. Lett. **91**(15), 153002 (2003).

24 I. A. Shkrob, M. C. Sauer, Jr., J. Phys. Chem. A **106**, 9120 (2002).

25 X. Chungeng, J. Peon, B. J. Kohler, Chem. Phys. **117**(19), 8855 (2002).

26 E. Gallicchio, B. J. Berne, J. Chem. Phys. **105**(16), 7064 (1996).

27 Z. Liu, B. J. Berne, J. Chem. Phys. **99**(11), 9054 (1993).

28 T. W. Kee, D. H. Son, P. Kambhampati, P. F. Barbara, J. Phys. Chem. A **105**(37), 8434 (2001).

29 I. B. Martini, E. R. Barthel and B. J. Schwartz, Science **293**, 462 (2001).

30 I. B. Martini, E. R. Barthel and B. J. Schwartz, J. Am. Chem. Soc. **124**, 7622 (2002).

31 D. R. Lide *Handbook of Chemistry and Physics, 85th Edition*, pages 12-17, (CRC Press, LLC, 2004).

32 E. A. Shaede, L. M. Dorfma, G. J. Flynn, D. C. Walker, Can. J. Chem. **51**, 3905 (1973).

33 J. Chandrasekhar, W. L. Jorgensen, J. Chem. Phys. **77**(10), 5073 (1982).

34 M. J. Bedard-Hearn, R. E. Larsen, B. J. Schwartz, J. Phys. Chem. B **107**(51), 14464-75 (2003).

35 P. M. Allen, D. J. Tildesely, *Computer Simulation of Liquids* (Clarendon Press, Oxford, 1987).

36 G. Ciccotti, M. Ferrario, J.-P. Ryckaert, Mol. Phys. **47**(6), 1253 (1982).

37 O. Steinhauser, Mol. Phys. **45**(2), 335 (1982).

38 W. L. Jorgensen, J. D. Madura, C. J. Swenson, J. Am. Chem. Soc. **106**(22), 6638 (1984).

39 J. Schnitker, P. J. Rossky, J. Chem. Phys. **86**, 3462 (1987).

40 F. Webster, P. J. Rossky, R. A. Friesner, Comp. Phys. Comm. **63**, 494 (1991).

41 A. Nobile, V. Roberto, Comp. Phys. Comm. **40**, 189 (1986); ibid., **42**, 233 (1986).

42 K. J. Drukker, Comp. Phys. **153**, 225 (1999).

43 C. J. Smallwood, W. B. Bosma, R. E. Larsen, B. J. Schwartz, J. Chem. Phys. **119**(21), 11263 (2003).

44 R. E. Larsen, B. J. Schwartz, J. Phys. Chem. B **108**(31), 11760 (2004).

45 M. J. Bedard-Hearn, C. J. Smallwood, R. E. Larsen, B. J. Schwartz, *in preparation*.

46 Note that the average energy of the solvated electron's ground state in methanol is calculated to be −1.5 eV in Ref. 16.

47 L. Turi, D. J. Borgis, Chem. Phys. **117**, 6186 (2002).

48 D. J. Bartels, Chem. Phys. **115**, 4404 (2001).

49 The distance between the centers of mass of the ground state and the fifth excited state is 10.9 Å, and the distance between the centers of mass of the ground state and the third excited state is 9.6 Å.

50 These calculations were performed for 1500 configurations of a neat THF simulation, where each configuration included in the average was separated by at least 20 fs. The details of the neat THF simulations are described in Ref. 34.

51 W. M. Bartczak,; K. Pernal, Comput. Chem. **24**, 469 (2000).

52 J. Schnitker, P. J. Rossky, G. A. Kenney-Wallace, J. Chem. Phys. **85,** 2986 (1986).

53 W. M. Bartczak, J. Kroh, M. Sopek, Radiat. Phys. Chem. **45**(6), 961 (1995).

54 K. A. Motakabbir, P. J. Rossky, J. Chem. Phys. **129**, 253 (1989).

55 J. J. Sakurai, *Modern Quantum Mechanics, Revised Edition* (Addison-Wesley Publishing Company, Menlo Park, 1994).

56 D. Borgis, A. Staib, Chem. Phys. Lett. **238**(1-3), 187 (1995).

57 In water, the density of energy differences and absorption spectrum match well because the three s-to-p-like transitions have nearly equal oscillator strength.

58 W.-S. Sheu, P. J. Rossky, J. Phys. Chem. **100**, 1295 (1996).

59 R. E. Larsen, B. J. Schwartz, *unpublished results*. The spherical harmonic projections were calculated using dynamically connected configurations over a 4.5-ps equilibrium trajectory of the solvated electron in water. The details of the simulation that produced these configurations are available in Ref. 43**.**

60 D. H. Son, P. Kambhampati, T. W. Kee, P. F. Barbara, J. Phys. Chem. A **105**(36), 8629 (2001).

61 http://www.cgl.ucsf.edu/chimera. C. C. Huang, G. S. Couch, E. F. Pettersen, T. E. Ferrin, "Chimera: An Extensible Molecular Modeling Application Constructed Using Standard Components." Pacific Symposium on Biocomputing **1**:724 (1996).

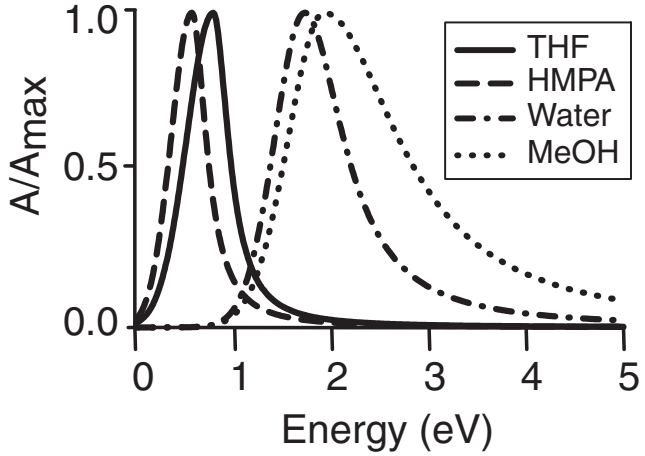

Figure 1
M. J. Bedard-Hearn, *et. al.*
For submission to the Journal of Chemical Physics

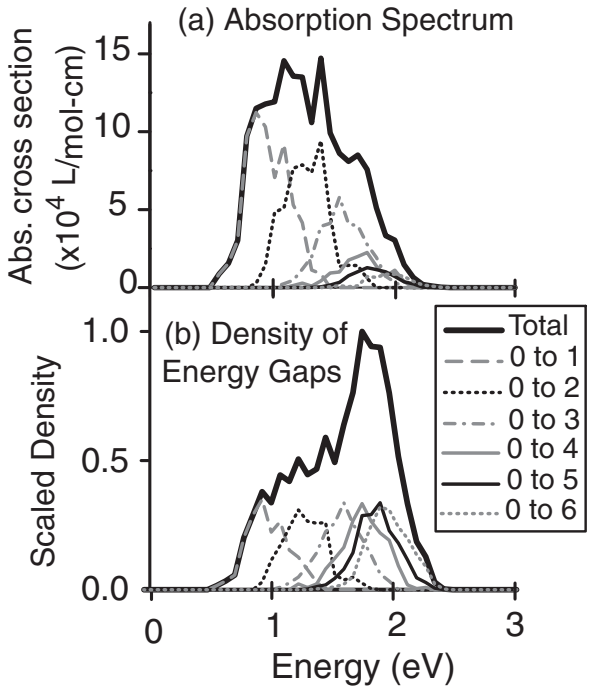

Figure 2
M. J. Bedard-Hearn, *et. al.*
For submission to the Journal of Chemical Physics

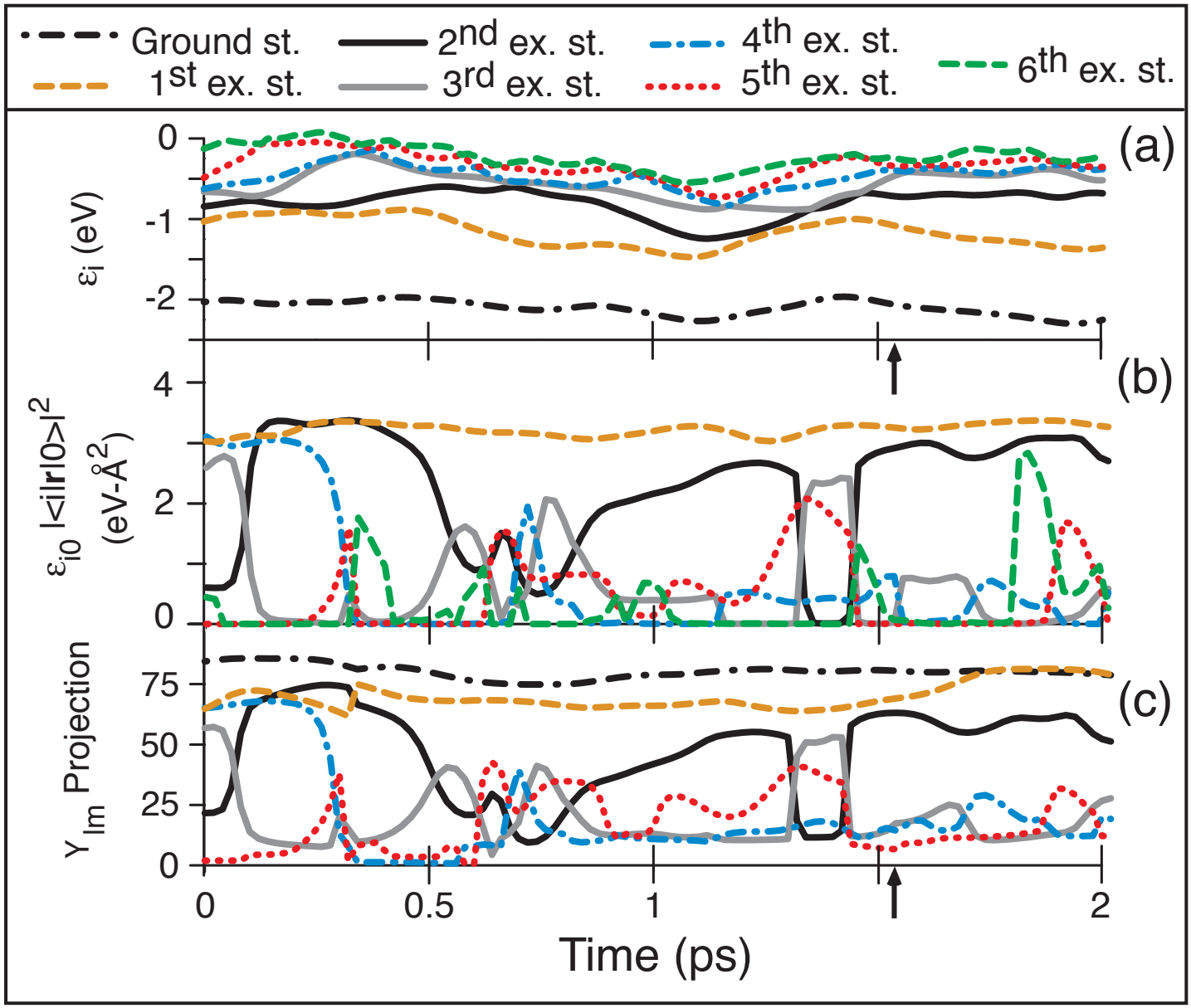

Figure 3 (color, two columns wide)
M. J. Bedard-Hearn, et. al.
For submission to the Journal of Chemical Physics

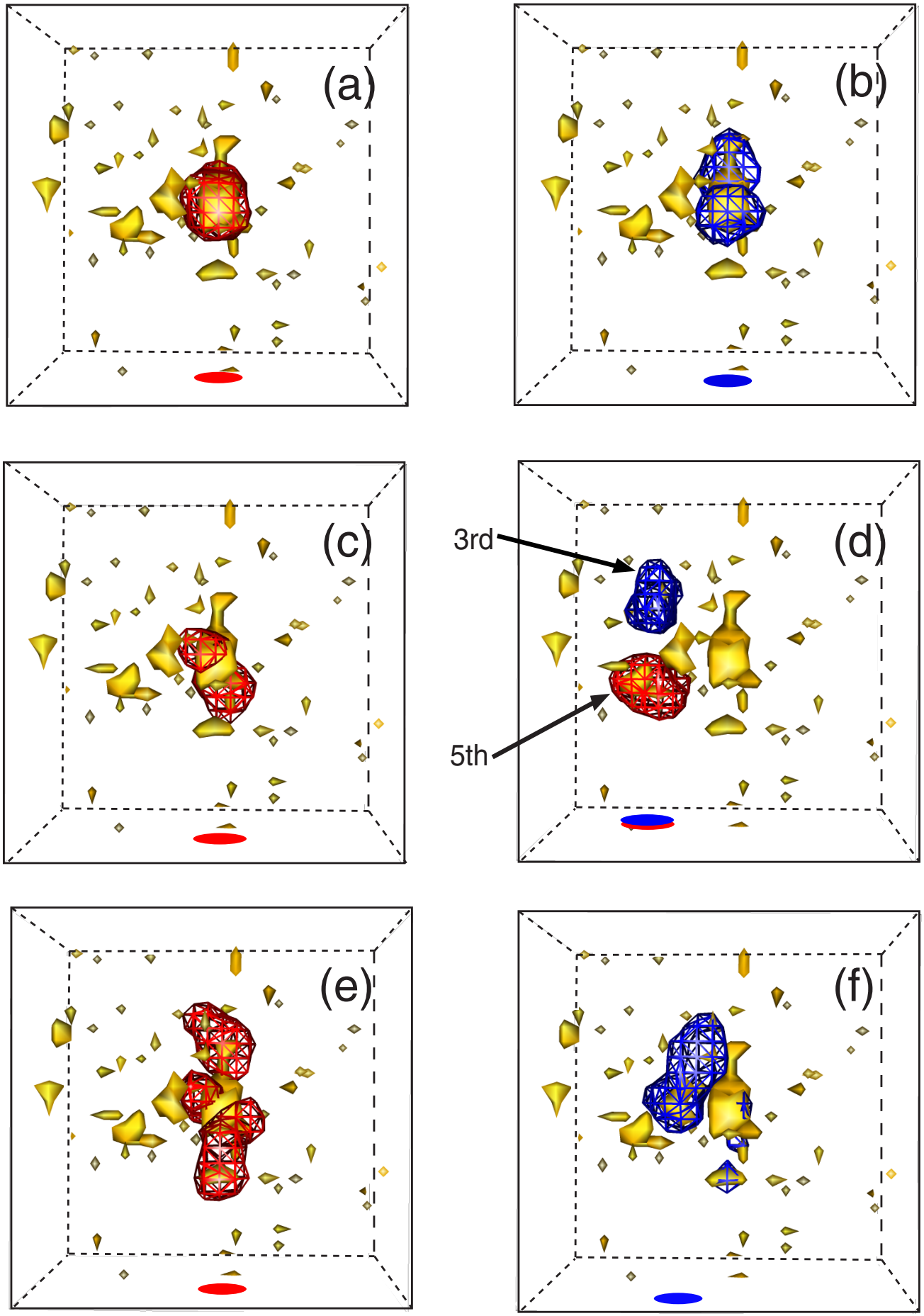

Figure 4 (color, full page) M. J. Bedard-Hearn, *et. al.* For submission to J. Chem. Phys.

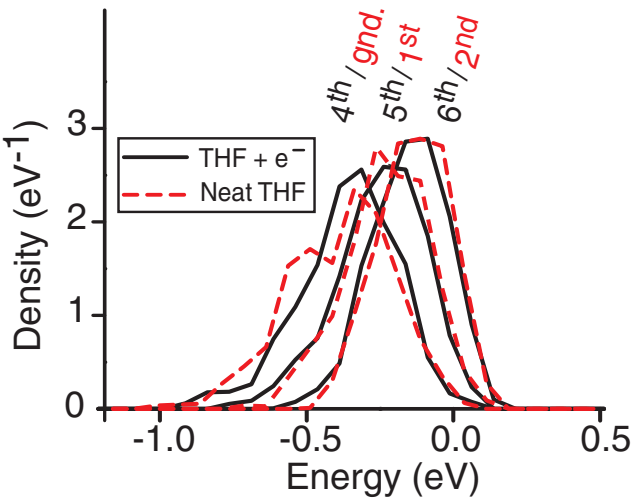

Figure 5 (color)
M. J. Bedard-Hearn, *et. al.*
For submission to the Journal of Chemical Physics